Chemistry–A European Journal
Review
doi.org/10.1002/chem.202301504
Chemistry Europe
European Chemical Societies Publishing
www.chemeurj.org

Materials for Electrochemiluminescence: TADF, Hydrogen-Bonding, and Aggregation- and Crystallization-Induced Emission Luminophores

Kenneth Chu,[a] Zhifeng Ding,*[a] and Eli Zysman-Colman*[b]

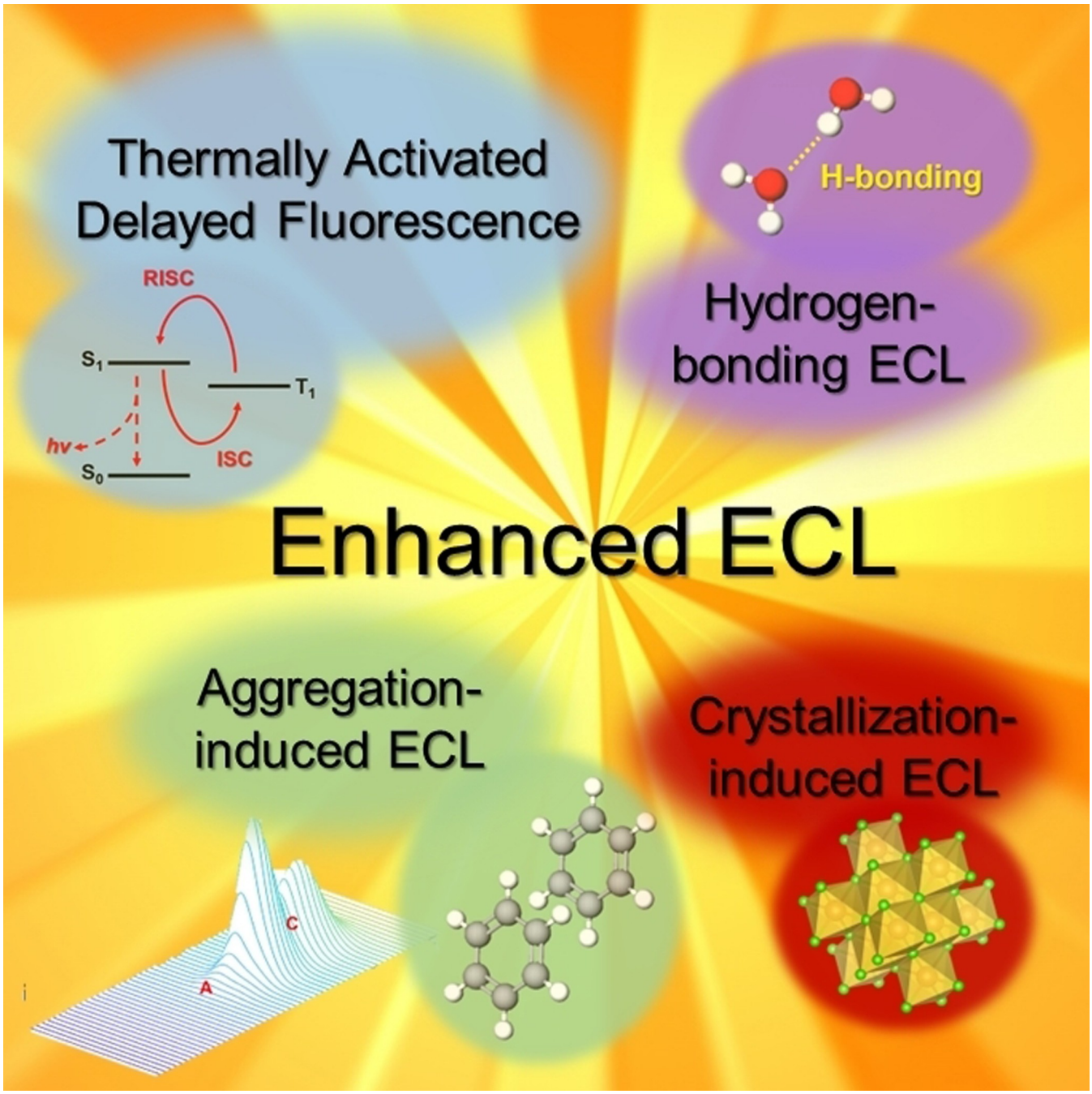

Electrochemiluminescence (ECL) is a rapidly growing discipline with many analytical applications from immunoassays to single-molecule detection. At the forefront of ECL research is materials chemistry, which looks at engineering new materials and compounds exhibiting enhanced ECL efficiencies compared to conventional fluorescent materials. In this review, we summarize recent molecular design strategies that lead to high efficiency ECL. In particular, we feature recent advances in the use of thermally activated delayed fluorescence (TADF) emitters to produce enhanced electrochemiluminescence. We also document how hydrogen bonding, aggregation, and crystallization can each be recruited in the design of materials showing enhanced electrochemiluminescence.

1. Introduction

Electrochemiluminescence (ECL) is the process by which electrogenerated radical species undergo electron transfer in the vicinity of a biased electrode to produce excitons (excited states); relaxation of these excited states produces ECL emission.[1] ECL has been exploited in biosensing,[2] single molecule detection,[3] light-emitting electrochemical cells (LECs),[4] and imaging[5] due to its high sensitivity, selectivity, and excellent signal-to-noise ratio. ECL can proceed via two mechanistic pathways. The annihilation pathway involves the generation of radical cations (holes) and radical anions (electrons) produced at the electrode from alternating oxidizing and reducing potentials, respectively. The electron transfer between these two electrogenerated radicals produces an exciton, which then can radiatively decay to produce the light. In the co-reactant route, the co-reactant, upon oxidation or reduction, can form a highly reactive intermediate that can interact with ECL luminophore polaron to produce the exciton. *n*-Tripropylamine (TPrA) is an example of an "oxidative-reductive" co-reactant, because upon oxidation, $TPrA^{\bullet+}$ deprotonates to form the TPrA radical ($TPrA^{\bullet}$), which is a strong reductant. On the other hand, benzoyl peroxide (BPO) is known as a "reductive-oxidative" co-reactant, as upon reduction and subsequent cleavage, the so formed benzoate radical ($PhCO_2^{\bullet}$) is strongly oxidizing. The use of co-reactants leads to enhanced ECL due to both the high oxidizing or reducing power of the reactive intermediates as well as their relatively high concentration compared to luminophore.[2,6] Organic long-persistent emission is characterized in compounds that remain luminescent for several seconds, even after the excitation source is removed. This phenomenon has been reported as organic long-persistent photoluminescence (OLPL) and electroluminescence (OLEL), particularly in TADF compounds that have large ΔE_{ST}.[7] More recently, this effect has also been observed in electrochemiluminescence (OLECL).[8]

The efficiency of an ECL reaction is defined as the ratio of the total number of photons produced by radiative relaxation of the electrically generated excitons to the total number of Faradaic electrons injected into the system.[1a] Until recently, the ECL efficiency of a system was reported relative to that of a well-known ECL luminophore, $[Ru(bpy)_3]^{2+}$ in the annihilation pathway or that of a $[Ru(bpy)_3]^{2+}$/co-reactant system. Methodologies to reproducibly and quantitatively determine the absolute ECL quantum efficiency have recently been made possible by us, utilizing on-demand calibrated detection systems such as photomultiplier tubes (PMTs),[9] photon-counting heads (PCHs) along with a spectrometer,[10] or a calibrated spectrograph/CCD camera array.[11] The accurate determination of the quantum efficiency of ECL luminophores is essential to assess the performance of the materials employed, as optimizing the photons-out/electrons-in ratio can represent significant cost savings for consumers. Enhancing the luminous efficiency of ECL processes can also improve the detection limit for sensing and imaging applications.

In general, the ratio of singlet to triplet excitons generated by recombination of Fermionic holes and electrons is 1:3 due to spin statistics.[12] Under electrical excitation this limits the maximum efficiency of fluorophores (compounds that are fluorescent) to 25%, since spin-forbidden transitions such as reverse intersystem crossing and radiative decay from the triplet state in the form of phosphorescence are slow and the triplet excitons are therefore prone to decay via alternative non-radiative relaxation pathways. In thermally activated delayed fluorescence (TADF) materials, in contrast, there is an efficient thermal up-conversion of triplet excitons to singlets, enabling the harvesting of both singlet and triplet excitons to produce light, and which unlike phosphorescent complexes, does not require the presence of a heavy metal to achieve internal quantum efficiencies up to 100%. For this reason, TADF material design has become extremely attractive in developing high efficiency emitters for electroluminescent devices, and by extension should be very promising in ECL applications. Other mechanisms, such as aggregation-induced electrochemiluminescence (AI-ECL), crystallization-induced electrochemiluminescence (CI-ECL), and hydrogen-bonding electrochemiluminescence (H-bonding ECL), can also be used to enhance the ECL efficiency. In contrast to TADF, which leverages the intrinsic photophysics properties of the emitting molecules to deliver enhanced emission, AI-ECL, CI-ECL, and H-bonding ECL utilize intermolecular interactions, that is, interactions between luminophore molecules, to result in enhanced emission.

[a] *K. Chu, Prof. Dr. Z. Ding*
Department of Chemistry, University of Western Ontario
London, ON N6A 5B7 (Canada)
E-mail: zfding@uwo.ca

[b] *Prof. Dr. E. Zysman-Colman*
Organic Semiconductor Centre
EaStCHEM School of Chemistry
University of St Andrews
Fife, KY16 9ST (UK)
E-mail: eli.zysman-colman@st-andrews.ac.uk

In this review, we summarize the new and emerging materials design strategies in developing high performance, high efficiency ECL luminophores. We focus on thermally TADF emitters, aggregated induced electrochemiluminescence (AI-ECL), crystallization induced electrochemiluminescence (CI-ECL), and hydrogen-bonding enhanced ECL.

2. Thermally Activated Delayed Fluorescence (TADF)

Phosphorescent molecules harvest both singlet and triplet excitons, converting the former into the latter by efficient intersystem crossing and then emit by phosphorescence, these processes mediated usually by the presence of a heavy atom that increases spin-orbit coupling. However, long excited-state lifetimes make triplet excitons prone to decaying by non-radiative pathways including by interacting with polarons or other excitons. Furthermore, phosphorescent materials usually incorporate expensive and scarce heavy metal elements such as ruthenium, platinum, or iridium. Molecules that emit via TADF are equally capable of harvesting both singlet and triplet excitons to produce light, but do not need the heavy elements. Functionally, TADF results from triplet excitons upconverting to singlets via reverse intersystem crossing (RISC) followed by radiative relaxation from S_1 to S_0. This process results in a delayed emission identical to the prompt fluorescence that also occurs from directly generated singlet excitons that radiatively decay, except it occurs on longer time scales. The efficiency of the TADF process is, to a first approximation, governed by the degree of spin-orbit coupling (ξ_{ST}) between the singlet and triplet excited states and the energy gap between them, ΔE_{ST} [Eq. (1)], where k_B is the Boltzmann constant and T is the temperature. Generally, as ΔE_{ST} decreases, the efficiency of the up-conversion process increases.

The magnitude of ΔE_{ST} is, in turn, determined by the exchange integral J, which describes the Coulombic repulsion between two electrons [Eq. (2)]. In other words, ΔE_{ST} will be small if the highest occupied molecular orbital (HOMO) and lowest unoccupied molecular orbital (LUMO) are spatially separated in the molecule.[13]

$$k_{RISC} \propto \xi_{ST}^2 e^{\left(\frac{-\Delta E_{ST}}{k_B T}\right)} \quad (1)$$

$$\Delta E_{ST} = 2J = 2 \int\int \phi_H(r_1)\phi_L(r_2)\frac{1}{|r_2 - r_1|}\phi_H(r_2)\phi_L(r_1)dr_1 dr_2 \quad (2)$$

The dominant strategy to spatially separate the HOMO and LUMO in an organic molecule is for it to adopt a highly twisted donor–acceptor geometry. In this context, the lowest lying excited state is one of charge-transfer (CT) character from the donor, where the HOMO is localized, to the acceptor, where the LUMO is localized. By selecting suitable D and A subunits, the HOMO/LUMO energy levels (and therefore the energy of the CT excited state) can be rationally tuned, providing compounds that emit from the ultraviolet to the near-infrared range. D-A

Kenneth Chu received his bachelor's degree from Western University in 2016, and following a brief stint working as an industry chemist, returned to complete his graduate studies under the supervision of Dr. Zhifeng Ding. He is currently in the final year of his PhD. His research interests include studying the electrochemistry and emission pathways of light (electro-chemiluminescence, electro-luminescence and chemiluminescence) for various materials including graphene quantum dots, metal alloy clusters and other materials and molecules.

Zhifeng Ding is a full professor of chemistry at Western University. He obtained his BSc in chemistry at Southeast University, MSc in coordination chemistry at Nanjing University and PhD in electrochemistry at the EPFL. He carried out his postdoctoral research at the University of Texas at Austin. His current research focuses on scanning electrochemical microscopy, ionic liquid electrolytes, solar cells and electro-chemiluminescence/electroluminescence/ chemiluminescence. His awards include Western Science Distinguished Research Professor (2014); Western University Faculty Scholar (2015-2016); Canadian Society for Chemistry McBryde Medal (2017); Ertl Prize (2018) and Chemistry Research Award of Excellence at Western (2023).

Eli Zysman-Colman obtained his Ph.D. from McGill University in 2003 under the supervision of Prof. David N. Harpp, conducting research in physical organic sulfur chemistry. He then completed two postdoctoral fellowships, one in supramolecular chemistry with Prof. Jay Siegel at the Organic Chemistry Institute, University of Zurich; the other in inorganic materials chemistry with Prof. Stefan Bernhard at Princeton University. He joined the Department of Chemistry at the Université de Sherbrooke in Québec, Canada as an Assistant Professor in 2007. In 2013, he moved to the University of St Andrews, where he is presently Professor of Optoelectronic Materials and Fellow of the Royal Society of Chemistry. His research focuses on the rational design of luminophores for energy-efficient visual displays and flat panel lighting based on OLEDs and light-emitting electrochemical cell devices; sensing materials for electrochemiluminescence; and developing photocatalysts for organic reactions.

architectures are not the only ones that can produce molecules/systems with small ΔE_{ST}. Through-space charge transfer (TSCT) emitters, multiresonant TADF (MR-TADF) emitters and exciplexes are all categories of materials that have been explored as emitters in electroluminescent devices.

2.1. Donor–acceptor TADF compounds

In 2014, Ishimatsu, Adachi, Imato and co-workers were the first to demonstrate ECL from donor-acceptor TADF emitters (2CzPN, 4CzPN, 4CzIPN, and 4CzTPN) in the annihilation pathway (Figure 1A).[14] These TADF molecules, incorporating carbazolyl and dicyanobenzene groups as donors and acceptors, respectively, demonstrated quasi-reversible reduction and irreversible multi-electron oxidation. The authors speculated that oxidation of these compounds could initiate polymerization (the polymer film on the electrode surface inhibits electrochemical activity) from the known unstable carbazole-centred radical cation. A small red-shift (ca. 10–20 nm) was observed when the solvent polarity was increased from DCM to MeCN (Figure 1B and C), due to the positive solvatochromism typically observed for compounds with CT emission. Furthermore, the authors observed a small red-shift between the ECL and PL emission, which was likely due to contributions from oligomers formed during the oxidation process in the ECL. They showed that **4CzIPN** could achieve a relative ECL efficiency of 50%, which both exceeded the 25% limit associated with fluorescent ECLphores imposed by spin statistics and approached the maximum efficiency dictated by the intrinsic photoluminescence quantum yield, Φ_{PL}, of the materials. Emission maxima, λ_{PL}, of 544 and 565 nm were reported in DCM and acetonitrile, respectively while the λ_{ECL} in these respective solvents were 555 and 565 nm. Since the PL and ECL spectra in MeCN matched for **4CzIPN**, the authors concluded that under ECL this compound showed TADF.

Our groups studied three D-A-TADF compounds **PPOCzPN**, **PPSCzPN**, and **DiPPOCzPN** (the molecular structures are displayed in the insets of Figure 2A, B, and C) for ECL, where the phosphine-chalcogenide modified carbazolyl donor groups stabilized the HOMO level to promote a blue-shifted emission (Figure 2).[8] Compounds **PPOCzPN**, **PPSCzPN**, and **DiPPOCzPN** emit at 498, 501, and 465 nm, respectively, in DCM. **DiPPOCzPN** showed the highest photoluminescence quantum yield, Φ_{PL}, of 61% of the three compounds. These three compounds demonstrated strong blue-green ECL emission in the presence of 10 mM BPO as the co-reactant (**PPOCzPN** $\lambda_{ECL}=520$ nm, **PPSCzPN** $\lambda_{ECL}=500$ nm, **DiPPOCzPN** $\lambda_{ECL}=545$ nm). In particular, **PPOCzPN** showed a 17% ECL efficiency relative to that of the reference $[Ru(bpy)_3]^{2+}$. Interestingly, we observed a delay in the ECL onset times, which we attributed to a phenomenon called organic long persistent ECL (OLECL), caused by a dissociation/association equilibrium between emissive excimer species and dissociated constituents. The magnitude of the ECL delay was also determined to be correlated with the ΔE_{ST}. For **PPOCzPN**, the ECL and PL emission matched, which indicates the same excited state was present in all pathways and suggests TADF behavior. In contrast, **PPSCzPN** and **DiPPOCzPN** displayed red-shifted ECL emission compared to their PL. This indicates likely exciplex involvement under the ECL conditions and may help to explain the decreased ECL efficiency when compared to **PPOCzPN**.

We also investigated the ECL behaviour of the TSCT TADF molecule **TPA-ace-TRZ** (Figure 3A).[15] This emitter produced ECL emission by both the annihilation and co-reactant pathways that was significantly red-shifted compared to the PL emission (Figure 3B). A significant delay in the ECL onset was seen (Figure 3C), which as observed with the inefficient D-A TADF emitters in Figure 2, hints at the formation of an exciplex. Exciplex formation is promoted by intermolecular excited CT states and typically also emit by TADF.[13] Using a standardized CCD camera/spectrograph instrument setup, the absolute ECL quantum efficiency of **TPA-ace-TRZ** was determined to be 0.028%, which was nine times stronger than that of the $[Ru(bpy)_3]^{2+}$ reference. Additionally, we explored the performance of **TPA-ace-TRZ** under a chemiluminescence pathway.

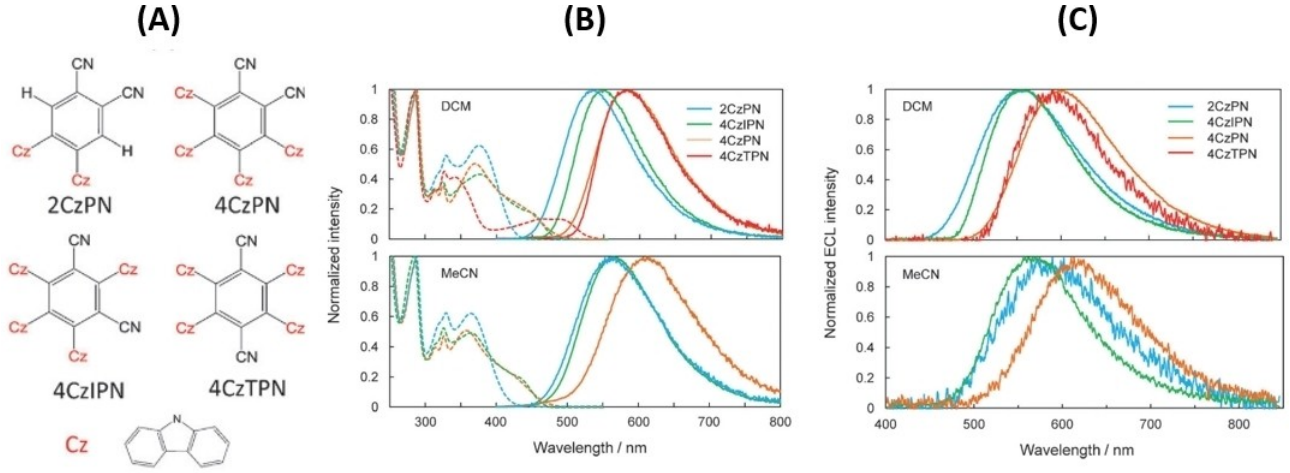

Figure 1. A) Molecular structures of **2CzPN**, **4CzPN**, **4CzIPN**, and **4CzTPN**. B) UV-Vis absorption (dotted) and PL spectra (solid lines) of 25 μM TADF emitter in DCM and MeCN. C) Normalized ECL spectra of TADF emitters in DCM and MeCN. Adapted with permission from ref. [14]. Copyright: 2014, Wiley-VCH.

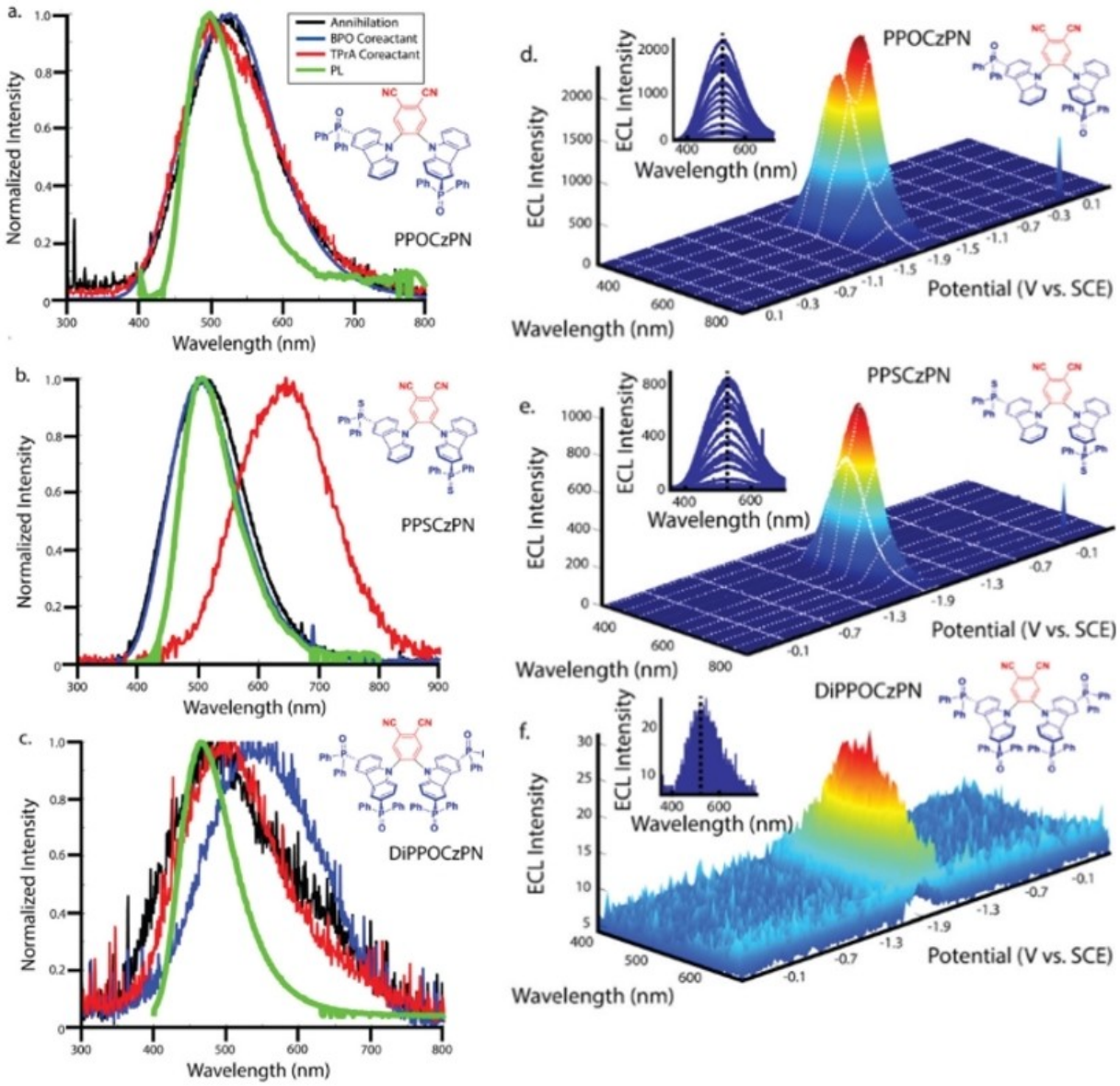

Figure 2. CVs (red) along with ECL-voltage curves (blue) during potential pulsing at a pulsing frequency of 10 Hz for A) **PPOCzPN**, B) **PPSCzPN** and C) **DiPPOCzPN**, all with 10 mM BPO added as a co-reactant D)–F) Spooling ECL spectroscopy of the corresponding systems. Insets in D)–F) represent stacked spooling ECL spectra. Adapted with permission from ref. [8]. Copyright: 2022, The Royal Society of Chemistry.

TPA-ace-TRZ produced bright yellow emission from the oxidation of the phenyl oxalate ester in the presence of hydrogen peroxide (Figure 3D). Notably, the emission wavelengths observed in PL, ECL, and CL spectra were all very close to each other, which strongly suggests the same exciplex excited state is present in all three pathways. Therefore, the interaction between **TPA-ace-TRZ** and high-energy intermediates formed from the CL reagents was proposed to form exciplexes, which is very uncommon in CL pathways.

Niu and co-workers reported ECL from a D-A TADF polymer **PCzAPT10** (Figure 4).[16] **PCzAPT10** displayed a broad PL at λ_{PL} of 508 nm in chlorobenzene, attributed to the emission of the TADF co-monomer chromophore. Using a glassy carbon **PCzAPT10**-modified electrode, they observed ECL under the TPrA co-reactant mechanism using MeCN as the solvent, where the ECL signal was red-shifted to 587 nm. The authors contended that the ECL electron-transfer processes could occur close to the **PCzAPT10**/MeCN solid/liquid interface, and therefore the so formed CT excitons located on the TADF co-monomer would be stabilized in the polar solvent. Due to the TADF nature of **PCzAPT10**, the ECL efficiency was enhanced fourfold compared to that of a fluorescent polymer standard F8BT, and two times to that of the $[Ru(bpy)_3]^{2+}$/TPrA system. The same group also studied the ECL behaviour of **4CzIPN** and the TSCT emitter **BPAPTC** in dichloromethane.[17] In this work, the authors were able to demonstrate ECL emission under both annihilation and co-reactant pathways, with a maximum ECL efficiency of approximately two times relative to $[Ru(bpy)_3]^{2+}$.

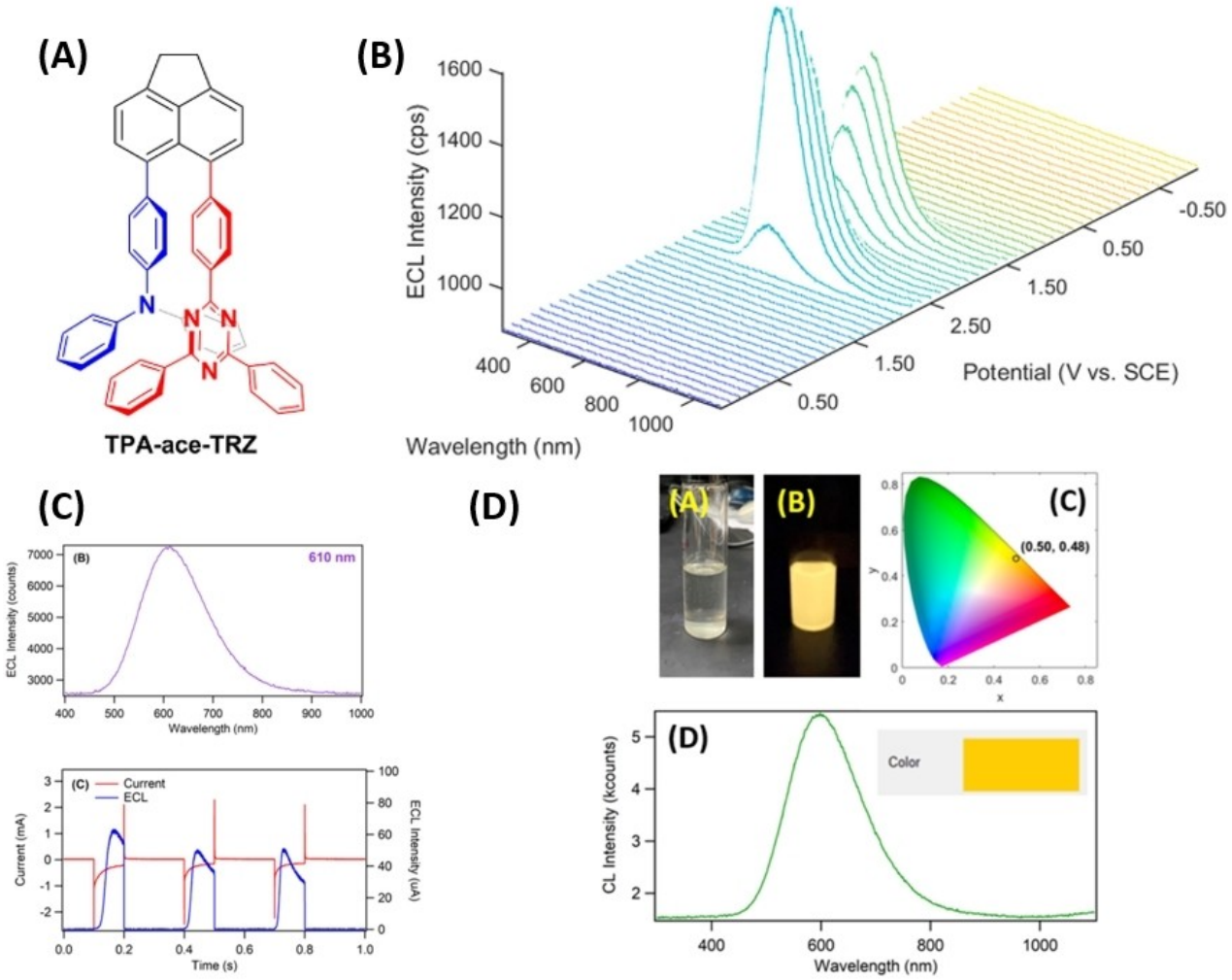

Figure 3. A) Structure of **TPA-ace-TRZ**. B) Spooling ECL spectra of **TPA-ace-TRZ** with 10 mM BPO as the co-reactant. C) Top: ECL accumulation spectrum of **TPA-ace-TRZ** with 10 mM BPO as the co-reactant; bottom: current–time and ECL-time profiles of **TPA-ace-TRZ** with the BPO co-reactant system. D) Left: Colour photographs of **TPA-ace-TRZ** CL reaction vial before/after adding H_2O_2; right: CIE colour coordinate diagram of **TPA-ace-TRZ** CL; bottom: CL accumulation spectrum of **TPA-ace-TRZ** system. Adapted with permission from ref. [15]. Copyright: 2023, American Chemical Society.

When compared to the results provided by Ishimatsu, Adachi, Imato and co-workers who investigated the ECL of **4CzIPN** in the annihilation pathway ($\lambda_{ECL} = 555$ nm), a red-shifted emission at 600 nm was observed for the **4CzIPN**-BPO co-reactant system. This red-shift in the ECL emission could be due to the increased reactivity of BPO to promote oligomerization and/or aggregated excited states. Due to the low oxidation potential of **BPAPTC**, an ECL onset potential as low as +0.46 V vs. Ag/AgCl was achieved. It was also confirmed that the PL and ECL spectra were very close for these two TADF luminophores under co-reactant pathways, providing strong evidence for TADF emission under ECL conditions. Niu et al. also reported a donor-acceptor TADF compound **PFSOTT5**, which demonstrated 5.79 times the ECL enhancement of a typical fluorescent polymer.[18]

TADF compounds have also been used in conjunction with other materials to produce enhanced ECL. Niu and co-workers encapsulated **4CzIPN** within an amphiphilic ethylene glycol based polymer (DSPE-PEG2000) to improve the water solubility for aqueous ECL applications.[19] The nano-encapsulated product displayed excellent stability and electrochemical reversibility, and demonstrated strong ECL emission in both annihilation and TPrA co-reactant pathways. Interestingly, the authors noted a small red-shift in the ECL emission compared to the PL, which they have attributed to involvement of molecular surface states, doubtless the effect of the nanoencapsulation strategy. **4CzIPN**, in this nano-encapsulated design, showed virtually the same PL characteristics as reported by the Ishimatsu, Adachi, Imato and co-workers ($\lambda_{PL} = 555$ nm), although the ECL emission was slightly red-shifted to 572 nm. The authors attributed this to the involvement surface states under electrochemical excitation.[20] The same group used a similar method to encapsulate instead conjugated TADF polymer dots (TADF-Pdots).[21] This report showed that the TADF-Pdots were capable of exhibiting the same ECL and PL emission at 510 nm, and showed a relative ECL efficiency in the TPrA co-reactant pathway of 11.73% vs. the $[Ru(bpy)_3]^{2+}$/TPrA reference system.

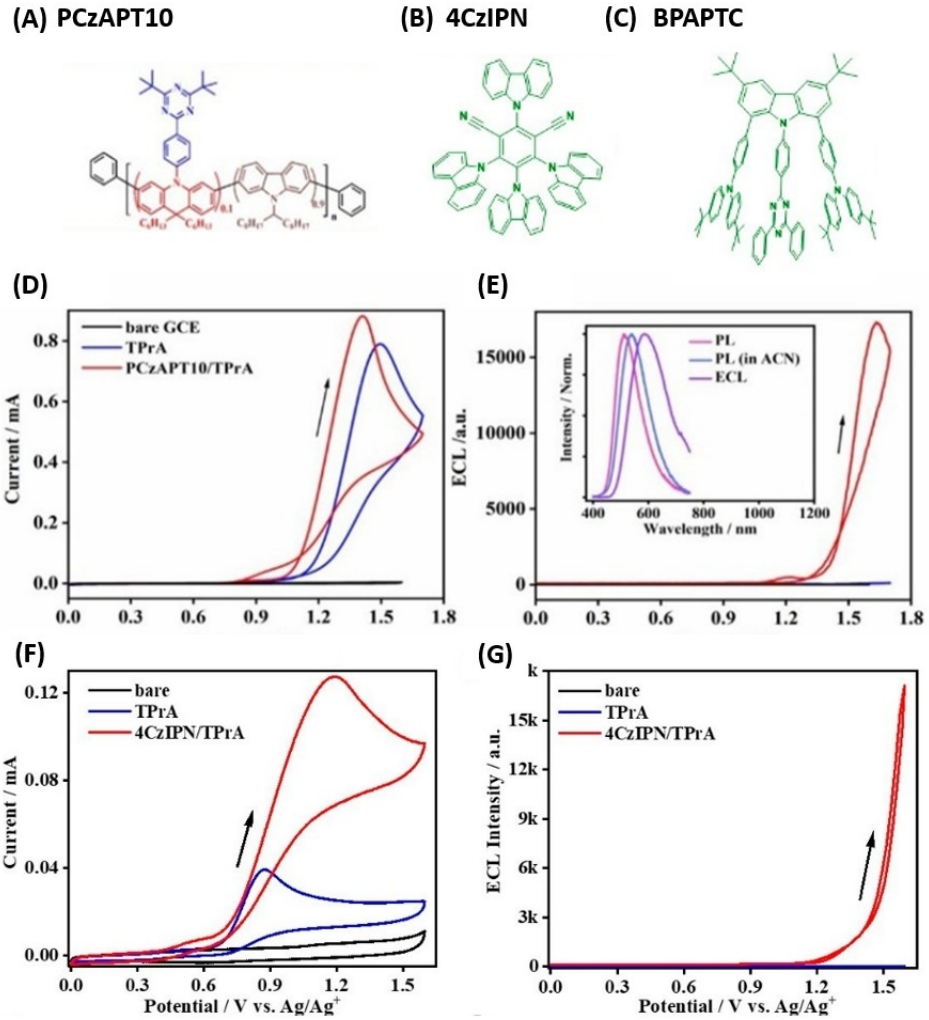

Figure 4. Chemical structures of A) **PCzAPT10** TADF polymer, B) **4CzIPN** and C) **BPAPTC** molecules. D) Cyclic voltammograms of **PCzAPT10**-modified GCE with TPrA. E) ECL–voltage curve of **PCzAPT10**. Inset: PL in neat film vs. MeCN, and ECL spectrum of the **PCzAPT10**/TPrA co-reactant system. F) Cyclic voltammograms and G) ECL–voltage curves of **4CzIPN** in dichloromethane with 0.1 M $TBAPF_6$ and 40 mM TPrA. Adapted with permission from refs. [16] and [17]. Copyright: 2021, Wiley-VCH.

Ju and co-workers improved significantly the Φ_{ECL} by creating Pdots using poly(TMTPA-DBC) as the TADF precursor.[22] The resulting TADF-Pdots showed very similar PL and ECL emission peaking at 517 and 520 nm, respectively, indicating that the same excited state was formed in the two pathways. As well, the Φ_{ECL} was enhanced up to 49.9% in the TPrA co-reactant system.

2.2. Multi-resonance (MR)-TADF compounds

As intimated earlier, another molecular design, first introduced by Hatakeyama et al. in 2016, is the MR-TADF emitter.[23] These compounds typically possess electron donor atoms and electron acceptor atoms that are arranged within a polycyclic aromatic hydrocarbon skeleton such that the HOMO and the LUMO are localized on alternating atoms, producing short-range CT (SRCT) excited states. This structure provides simultaneously a sufficiently small ΔE_{ST} to promote TADF while suppressing molecular vibration, leading to narrowband emission and high Φ_{PL}.[24]

Our research groups reported the MR-TADF emitter **Mes_3DiKTa** (Figure 5A), which has a ΔE_{ST} of 0.26 eV and high Φ_{PL} of 80% at 3.5 wt.% doped films in 1,3-bis(*N*-carbazolyl)benzene (mCP), and studied its ECL behaviour in acetonitrile.[25] Strong ECL was detected for this compound in the presence of TPrA as a co-reactant, with a relative efficiency of 79% recorded at a TPrA concentration of 20 mM versus $[Ru(bpy)_3]^{2+}$. Both delayed onset (about 5 ms after the application of potential) and slow decay (~10 ms after the applied potential returns to 0 V) of the ECL reaction were observed in the potential pulsing experiment where the ECL emission could be monitored with respect to the potential steps (Figure 5B). This may be due to OLECL, a process that involves the charge separation and slow recombination in exciplexes that may be particularly relevant to systems with a moderate ΔE_{ST}. However, competing processes for delayed emission including TTA and TADF could not be completely ruled out in this instance. The

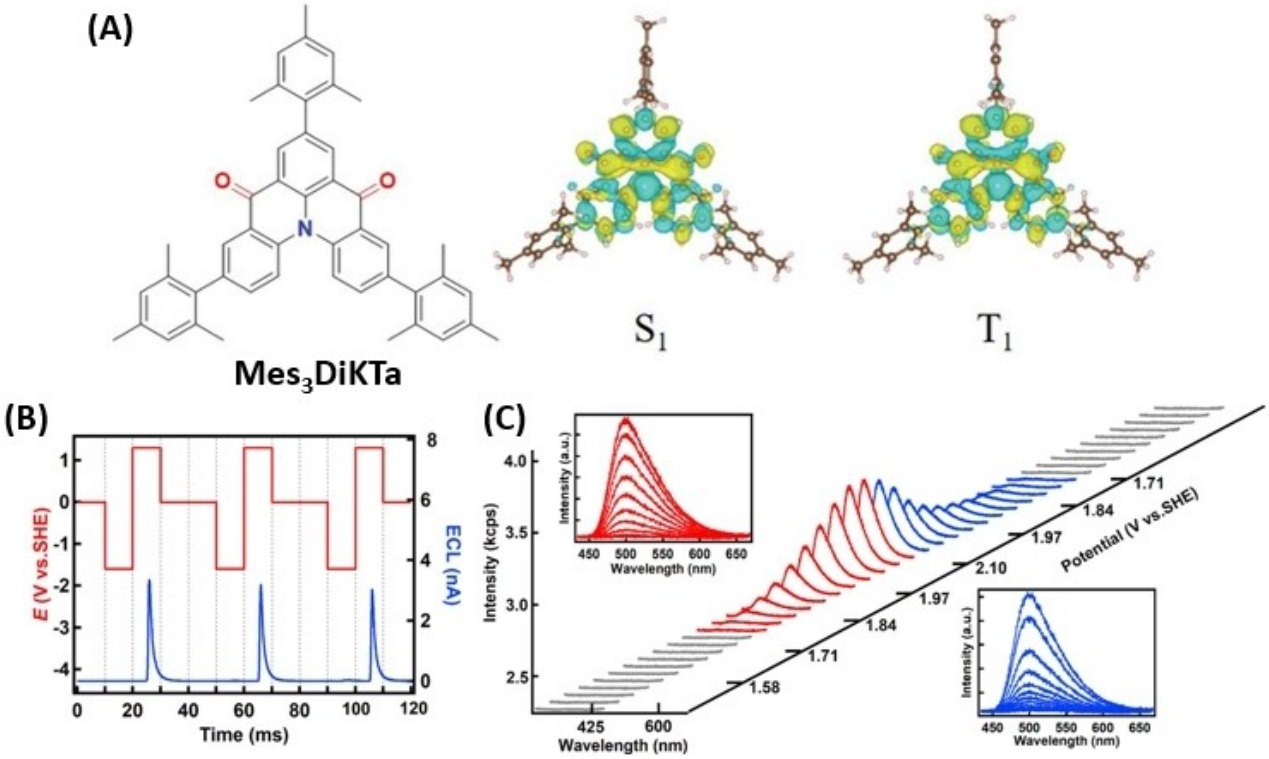

Figure 5. A) Structure and calculated difference density plots of **Mes_3DiKTa**. B) Time-resolved ECL experiments with 0.2 mM **Mes_3DiKTa** in acetonitrile by the annihilation pathway. C) Spooling ECL spectra of 0.2 mM Mes_3DiKTa in the presence of 20 mM TPrA as a co-reactant, with a scan rate of 0.02 $V\,s^{-1}$ and exposure time of 2 s. Adapted with permission from refs. [25a] and [25b]. Copyright: 2020, Wiley-VCH and 2023, IOP Publishing.

presence of OLECL was also proposed to enhance the overall ECL emission; accordingly, the absolute ECL efficiencies of **Mes_3DiKTa** were determined to be 0.0013% in the annihilation route and 1.1% in the TPrA co-reactant system. Using spooling ECL spectroscopy (Figure 5C), we identified that a combination of monomer and aggregate excited states contributed to the ECL emission.

Of the three systems reported for OLECL, there appears to be a direct correlation between the magnitude of ΔE_{ST} and the delayed onset time in the ECL: the compound with the smallest ΔE_{ST} (**TPA-ace-TRZ**, $\Delta E_{ST} = 0.06$ eV) also displayed the longest delay onset (25 ms) and persistent emission (57 ms), while **Mes_3DiKTa** ($\Delta E_{ST} = 0.26$ eV) and PPOCzPN ($\Delta E_{ST} = 0.21$ eV) had shorter delay onsets, 5 and 7 ms, respectively. While additional verification is required, these results suggest that a small ΔE_{ST} may promote delayed emission following the OLECL pathway. Furthermore, this indicates that the engagement of OLECL and exciplex formation may be a competing mechanism to TADF.

3. Hydrogen Bonding System ECL

Hydrogen bonding between ECL luminophores is another strategy to produce enhanced electrochemiluminescence. This bonding interaction to create self-assemblies could effectively restrict intramolecular rotation to enhance ECL in an alternative pathway towards aggregation-induced emission. For example, hydrogen bond organic frameworks (HOFs) can be self-assembled from organic ligands using hydrogen bonding interactions. HOFs can facilitate the aggregation of molecular luminophores that result in AIE, which is then exploited to produce enhanced ECL.[26] Among other strategies to enhance ECL, favourable hydrogen bonding (H-bonding) interactions between the emitter and secondary compounds could both promote ECL activity by pre-organization and stabilize the ECL. Our groups studied the H-bonding interaction between an Ir^{III} complex (**1**) and pyrimido-[4,5-c]isoquinolin-3-amine (**3**), and its effects on the ECL (Figure 6).[27] In electrochemical measurements, the H-bonding complex of [**1**·**3**] showed additional reduction signals that were not present in either precursor. The [**1**·**3**] adduct also showed enhanced multi-peak ECL emission with BPO as a co-reactant, with emission peaks originating from a combination of exciplexes between **1**, **3**, and BPO radicals. The addition of DMF to suppress H-bonding also significantly changed the electrochemical and ECL properties, revealing a highly dynamic ECL environment.

H-bonding can also play a more structural role in enhancing ECL. You et al. showed that a $[Ru(dcbpy)_3]^{2+}$/carbon quantum dot (CQD) matrix could act as an effective sensing platform, where the H-bonding facilitated electron transfer due to the decreased intermolecular distance between emitter and co-reactant.[28] The authors speculated that H-bonds could form between oxygen-rich functional groups, and this effect was confirmed by an enhancement in the electrochemical oxidation

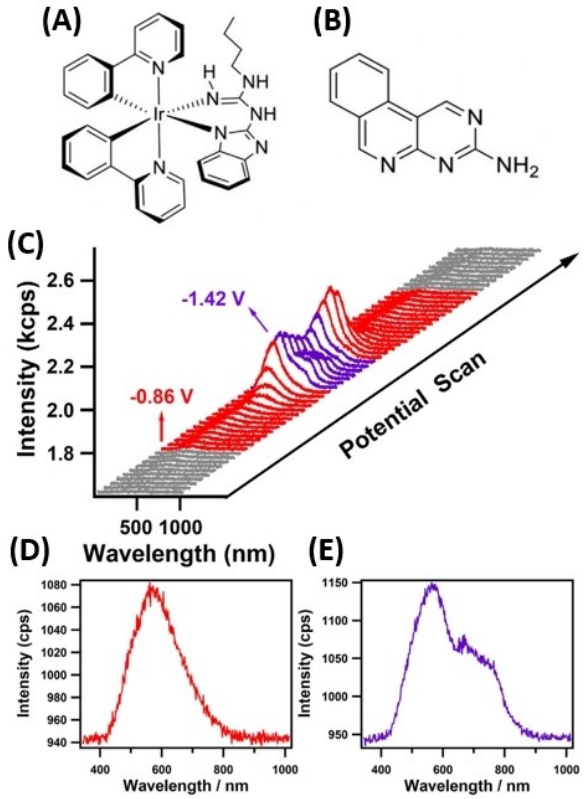

Figure 6. A) Chemical structures of Ir^{III} complex [**1**] and B) pyrimido-[4,5-c]isoquinolin-3-amine [**3**], which combine through H-bonding to form complex [**1·3**]. C) Spooling ECL spectra of complex [**1·3**] with 5 mM BPO as co-reactant. ECL spectra at D) −1.34 and E) −1.50 V. Adapted with permission from ref. [27]. Copyright: 2022, Elsevier B.V.

current of the $[Ru(dcbpy)_3]^{2+}$/CQD composite vs. the unmodified electrode. This H-bonded composite showed an ECL emission at 660 nm, which closely matched its PL emission. Using this platform, they were able to successfully realize the detection of 17-β estradiol (B2) at micromolar concentrations.

Feng et al. demonstrated that a self-assembled triazinyl-based hydrogen bond organic framework (**Tr-HOF**) constructed from 2,4-diaminotriazinyl (phenyDAT) could achieve an enhanced ECL compared to that using the individual phenyDAT monomers.[29] The three-dimensional structure of the **Tr-HOF** is stabilized by N···H hydrogen bonds, suppressing the quenching effects of ligand π–π stacking while simultaneously providing large active surface area for efficient electron transfer (Figure 7). This unique system attained 21% ECL efficiency relative to $[Ru(bpy)_3]^{2+}$, which was a substantial improvement from monomeric phenyDAT. **Tr-HOF** demonstrated an ECL emission at 643 nm that is red-shifted by 10 nm from its PL emission, which the authors asserted was due to emission from different excited states in the two processes. In a similar vein, Lei et al. assembled two kinds of HOFs, **HOF-101** and **HOF-100** using 1,3,6,8-tetra(4-carboxylphenyl)pyrene and 1,3,6,8-tetracarboxypyrene, respectively.[30] **HOF-101** demonstrated an effect termed intra-reticular electron coupling (IREC), which improves long-range charge transfer.[31] **HOF-101** displayed very similar PL and ECL emission in aqueous solution at 502 and 503 nm, respectively. IREC was thought to contribute to an enhancement in the ECL efficiency up to 64.7% vs. $[Ru(bpy)_3]^{2+}$ when using TPrA as a co-reactant. Importantly, the authors also noted that the stacking morphology driven by intermolecular and intramolecular H-bonds could have a significant impact on the charge transfer (and therefore ECL) capabilities.

4. Enhanced ECL from AIE and CIE

In 2011, Tang et al. introduced the concept of aggregation induced emission (AIE), where they observed the unprecedented enhancement of emission upon molecular aggregation in siloles. The intramolecular rotation of phenyl "rotors" in hexaphenylsilole (HPS) serves to quench the excited state through non-radiative decay. Suppression of this effect via restriction of intramolecular rotation (RIR) therefore enhances the emission of the aggregated state.[32] The combination of AIE and ECL, termed aggregated induced electrochemiluminescence (AIECL), focuses on the smart design of ECL luminophores that can simultaneously exploit the AIE mechanism.[33] The first example of AI-ECL was reported by de Cola et al., who explored the formation of supramolecular structures of Pt^{II} complexes.[34] Since this work, there have been numerous advances in this area of research. Crystallization-induced emission (CIE) is based upon the same principle as AIE – the restriction of intramolecular rotation to block the non-radiative emission pathways – by means of lattice formation.[35] CIE luminophores demonstrate enhanced emission from crystallization, but not amorphization.[36] In CIE, the molecular structure, conformation, and morphological packing all play an important role in enhancing the emission. Solvent fuming, which is a technique to induce crystallization in chromophores, can be used as a reversible method to attain crystallization-induced electrochemiluminescence (CI-ECL). Significant enhancement to the ECL efficiency is possible with CIE luminophores.

4.1. Aggregation-induced electrochemiluminescence (AIECL)

Ye et al. designed a cyclometalated iridium(III) complex for AIECL.[37] AIE behaviour was confirmed with increasing H_2O content during the ECL acquisition, as demonstrated in Figure 8. This iridium(III) complex showed strong PL emission at 643 nm, which closely matched its ECL emission at 640 nm in dimethylsulfoxide (DMSO)/water using TPrA as the co-reactant. The authors were able to demonstrate a 39-fold enhancement in the ECL efficiency compared to the monomolecular state, and fourfold enhancement compared with the $[Ru(bpy)_3]^{2+}$ reference. In a related work, Wei et al. encapsulated *fac*-Ir(ppy)$_3$ in apoferritin (apoFt), creating an Ir(ppy)$_3$@apoFt bioconjugate. Through pH-controlled reversible dissociation of apoFt subunits[38] and analysis using optical emission spectroscopy, the authors were able to confine, on average, 44.3 molecules of *fac*-Ir(ppy)$_3$ into the cavity of the protein core, effectively restricting intramolecular movement to produce AIECL.[39] Using

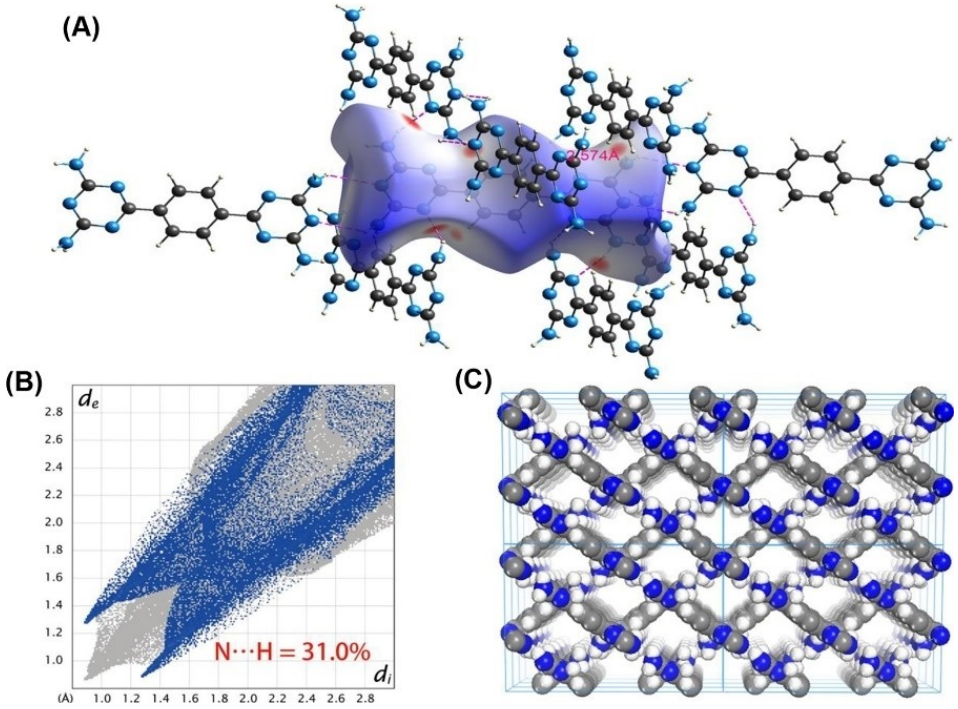

Figure 7. A) Intermolecular interactions of **phenyDAT** in Tr-HOFs with the labelled distance extracted from its crystal packing data. B) View of the Hirshfeld surface mapped over the normalized distance of the N···H bond for **phenyDAT** in Tr-HOFs. C) 3D packing framework of Tr-HOFs. Reproduced with permission from ref. [29]. Copyright: 2021, American Chemical Society.

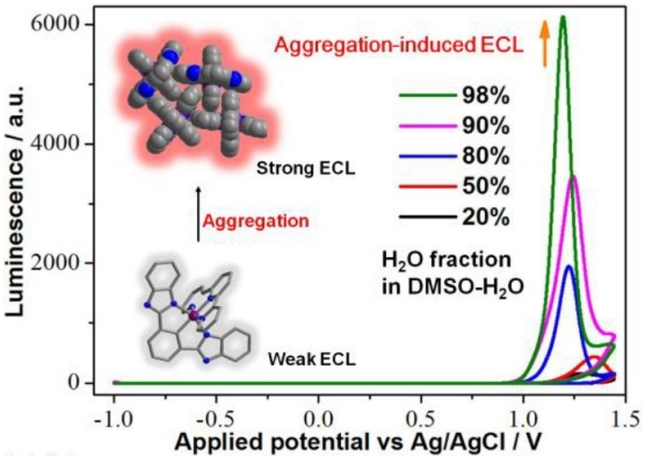

Figure 8. ECL intensity variation as the H_2O fraction of a DMSO/H_2O solvent mixture is increased. Reproduced with permission from ref. [37]. Copyright: 2018, American Chemical Society.

TPrA as a co-reactant, the authors demonstrated enhanced PL (565 nm), ECL (531 nm), and electrochemical activity of the aggregates compared to the monomers. The ECL emission was blue-shifted compared to the PL, possibly due to the RIR effect afforded by AIE, wherein the blocking of non-radiative energy loss promotes a higher energy emission wavelength. This effect may be related to the crystallization-induced blue-shift (CIBS) observed by Tang and co-workers.[36,40] They were also able to use $Ir(ppy)_3$@apoFt to construct an immunosensor for CYFRA-21 (a cancer cell biomarker) detection, attaining a wide linear response range and a low detection limit.

Xu et al. studied the AIECL properties of carboranyl carbazoles (Figure 9A).[20] These metal-free "organic dots" were weakly emissive until the water fraction reached over 85%, at which point their emission intensity dramatically increased (Figure 9B). Their model compound **T-3** exhibited slightly red-shifted ECL emission (582 nm) compared with their PL emission (547 nm), which the authors have attributed to surface-state transitions, which are commonly accessed in ECL pathways. The morphology and the size of the carboranyl carbazole aggregates were also found to have a significant influence on the AIE and ECL character of this luminophore. **T-3** displayed a 20-fold enhancement in the ELC performance when compared to the reference compound without AIE behaviour.

An example of aggregation-induced delayed fluorescence electrochemiluminescence (AIDF-ECL) was reported by Niu and co-workers. They tested **mCP-BP-PXZ**, which was a known AIDF luminophore, and compared it to **TPE-TAPBI**, a reference AIECL luminophore. **mCP-BP-PXZ** displayed a 5.4-fold stronger ECL signal when tested in thin-film modified GCE in the presence of TPrA as the co-reactant versus the **TPE-TAPBI** reference, which the authors rationalized as due to effective utilization of triplet excitons generated during the electrochemical excitation.[41] Also, the ECL spectrum (596 nm) was red-shifted by 53 nm versus the PL spectrum (543 nm), which may be due to the involvement of surface-state transitions that are commonly observed in semiconductor type ECL emitters.

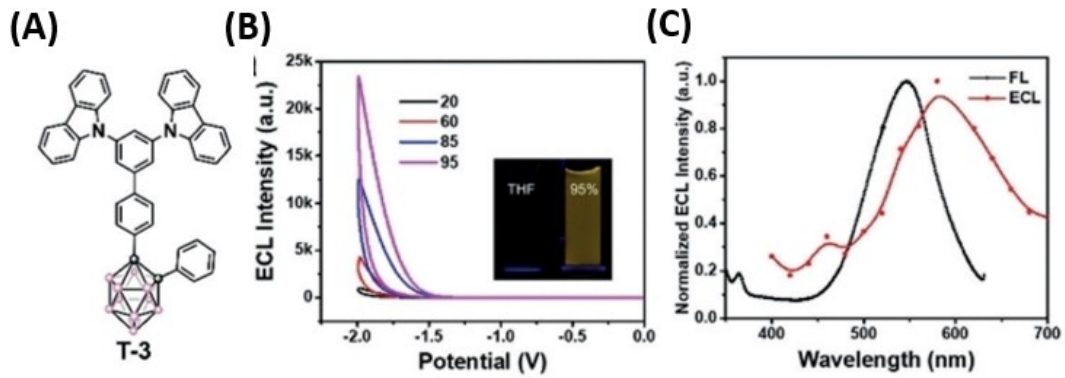

Figure 9. A) Molecular structure of the carboranyl carbazole AI-ECL luminophore. B) ECL intensity of 1.0 mM T-3 in increasing H_2O fractions. C) PL spectrum of T-3 in 95 % H_2O (black) and ECL spectrum of T-3 modified GCE in 95 % H_2O (red). Reproduced with permission from ref. [20]. Copyright: 2019, Wiley-VCH.

4.2. Crystallization-induced electrochemiluminescence (CIECL)

This effect in ECL was first documented by the Wang, Ding and co-workers who studied a di-boron complex (DBC).[42] Using PL and X-ray diffraction techniques, they were able to unambiguously observe crystallization induced blue-shifted (CIBS) emission as well as enhanced PL emission in the crystalline state (Figure 10). A strong increase in the ECL activity was also recorded, particularly in the BPO co-reactant pathway, when using glassy carbon electrodes modified with DBC (fivefold enhancement in the crystalline film versus the solution phase). Finally, through the use of spooling ECL spectroscopy,[43] it was discovered that ECL reactions can occur at different locations following annihilation and co-reactant pathways, where in the DBC/BPO system the ECL reactions are confined predominantly at the solid-solution interface.

More recently, Zhu and co-workers created a $[Ru(bpy)_3]^{2+}$ derivative **Ru-TPE**, incorporating the AIE-active tetraphenylethene (TPE) group.[44] The resulting compound exhibited strong CIECL driven by the TPE group that overcame the inherent ACQ nature of $[Ru(bpy)_3]^{2+}$. The authors observed an increased crystallinity of the **Ru-TPE** crystals compared to plain crystals of

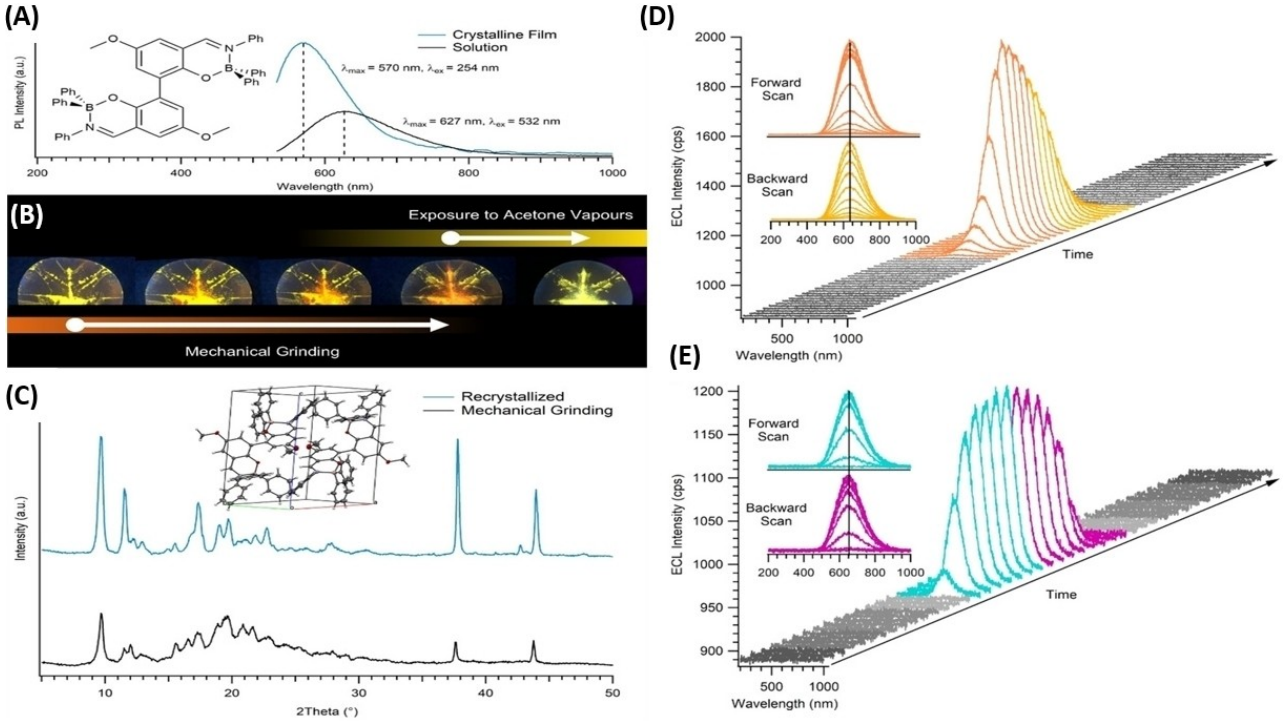

Figure 10. A) PL spectra of a crystalline DBC film (blue) and DBC in acetonitrile (black). B) Images of recrystallized DBC, DBC after mechanical grinding, and DBC after exposure to acetone vapour (left to right). C) XRD spectra of recrystallized DBC (blue) and DBC upon grinding (black); inset: DBC unit cell. Spooling ECL spectra of D) solid state ECL/BPO co-reactant and. E) homogeneous DBC/BPO systems. Reproduced with permission from ref. [42]. Copyright: 2020, Wiley-VCH.

$[Ru(bpy)_3]^{2+}$, confirmed by pXRD measurements. By using an ITO/Ru-TPE modified electrode, where the ECL emission originated from a solid-state film, an impressive ECL efficiency of 236% vs. the $[Ru(bpy)_3^{2+}]$/TPrA reference system (in the solution state) was recorded. **Ru-TPE** showed an ECL at 631 nm, red-shifted by 30 nm from its PL emission (601 nm), which suggests that the emissive excited state of **Ru-TPE** may originate from surface-state transitions.

5. Conclusion and Outlook

Enhanced electrochemiluminescence continues to be one of the perpetual targets for researchers as evidenced by the rapid growth in ECL applications and technologies. The landscape of ECLphores and strategies to promote ECL have rapidly expanded in recent years. In this review, we have summarized, for the first time, the advances in materials that have resulted in greatly enhanced electrochemiluminescence efficiencies. In particular, TADF materials have ushered in a new era of high-performance ECL luminophores. Several challenges in ECL research related to those involving TADF luminophores remain, including improving the ECL efficiency to levels similar to those observed in electroluminescent devices. It is possible that the more complex mechanisms of ECL, particularly the co-reactant pathways, suffer from an increased likelihood of non-radiative decay, reducing the overall luminous efficiency. In a related avenue, the ECL mechanistic pathways involving TADF ECL molecules have not as of yet been fully elucidated and they will be fundamental to understanding how to improve ECL efficiencies. Finally, using a standardized method to report absolute ECL efficiencies will be an enormous improvement to the field when assessing the performance of new ECL luminophores. It is evident that there is still much chemical space and opportunity to explore to produce materials with enhanced ECL and also that the future is bright for the design of smart ECL materials.

Acknowledgements

We thank the Natural Sciences and Engineering Research Council Canada (NSERC, DG RGPIN-2018-06556, DG RGPIN-2023-05337 and SPG STPGP-2016-493924), New Frontiers in Research Fund (NFRFR-2021-00272), Canada Foundation of Innovation/Ontario Innovation Trust (CFI/OIT, 9040) and The University of Western Ontario for the support to this research. KC is an Ontario Graduate Scholar. We are grateful also to the quality service from our Electronic Shop in Chemistry, Glass Shop and ChemBioStores at University of Western Ontario.

Conflict of Interests

The authors declare no conflict of interest.

Data Availability Statement

Data sharing is not applicable to this article as no new data were created or analyzed in this study.

Keywords: absolute ECL quantum efficiency · aggregation-induced emission · crystallization-induced emission · electrochemiluminescence · hydrogen bonding · thermally activated delayed fluorescence

[1] a) M. M. Richter, *Chem. Rev.* **2004**, *104*, 3003–3036; b) M. Hesari, Z. Ding, *J. Electrochem. Soc.* **2016**, *163*, H3116-H3131.
[2] a) W. Miao, A. J. Bard, *Anal. Chem.* **2004**, *76*, 7109–7113; b) N. Egashira, S.-i. Morita, E. Hifumi, Y. Mitoma, T. Uda, *Anal. Chem.* **2008**, *80*, 4020–4025; c) D. Tian, C. Duan, W. Wang, N. Li, H. Zhang, H. Cui, Y. Lu, *Talanta* **2009**, *78*, 399–404.
[3] a) A. J. Bard, F.-R. F. Fan, *Acc. Chem. Res.* **1996**, *29*, 572–578; b) J. Dong, Y. Lu, Y. Xu, F. Chen, J. Yang, Y. Chen, J. Feng, *Nature* **2021**, *596*, 244–249; c) Y. Lu, X. Huang, S. Wang, B. Li, B. Liu, *ACS Nano* **2023**, *17*, 3809–3817.
[4] a) K. Chu, J. R. Adsetts, C. Moore, Z. Ding, *ACS Appl. Electron. Mater.* **2020**, *2*, 3825–3830; b) J. R. Adsetts, R. Zhang, L. Yang, K. Chu, J. M. Wong, D. A. Love, Z. Ding, *Front. Chem.* **2020**, *8*, 865.
[5] a) G. Valenti, S. Scarabino, B. Goudeau, A. Lesch, M. Jović, E. Villani, M. Sentic, S. Rapino, S. Arbault, F. Paolucci, N. Sojic, *J. Am. Chem. Soc.* **2017**, *139*, 16830–16837; b) H. Zhang, Y. Liu, M. Yao, W. Han, S. Zhang, *Anal. Chem.* **2023**, *95*, 570–574; c) X. Huang, B. Li, Y. Lu, Y. Liu, S. Wang, N. Sojic, D. Jiang, B. Liu, *Angew. Chem. Int. Ed.* **2023**, *62*, e202215078.
[6] a) W. Miao, *Chem. Rev.* **2008**, *108*, 2506–2553; b) L. Li, Y. Chen, J.-J. Zhu, *Anal. Chem.* **2017**, *89*, 358–371.
[7] a) W. Li, Z. Li, C. Si, M. Y. Wong, K. Jinnai, A. K. Gupta, R. Kabe, C. Adachi, W. Huang, E. Zysman-Colman, I. D. W. Samuel, *Adv. Mater.* **2020**, *32*, 2003911; b) K. Jinnai, N. Nishimura, C. Adachi, R. Kabe, *Nanoscale* **2021**, *13*, 8412–8417.
[8] S. Kumar, P. Tourneur, J. R. Adsetts, M. Y. Wong, P. Rajamalli, D. Chen, R. Lazzaroni, P. Viville, D. B. Cordes, A. M. Z. Slawin, Y. Olivier, J. Cornil, Z. Ding, E. Zysman-Colman, *J. Mater. Chem. C* **2022**, *10*, 4646–4667.
[9] J. R. Adsetts, K. Chu, M. Hesari, J. Ma, Z. Ding, *Anal. Chem.* **2021**, *93*, 11626–11633.
[10] K. Chu, J. R. Adsetts, J. Ma, C. Zhang, M. Hesari, L. Yang, Z. Ding, *J. Phys. Chem. C* **2021**, *125*, 22274–22282.
[11] J. R. Adsetts, K. Chu, M. Hesari, Z. Whitworth, X. Qin, Z. Zhan, Z. Ding, *J. Phys. Chem. C* **2022**, *126*, 20155–20162.
[12] M. Y. Wong, E. Zysman-Colman, *Adv. Mater.* **2017**, *29*, 1605444.
[13] H. Nakanotani, Y. Tsuchiya, C. Adachi, *Chem. Lett.* **2021**, *50*, 938–948.
[14] R. Ishimatsu, S. Matsunami, T. Kasahara, J. Mizuno, T. Edura, C. Adachi, K. Nakano, T. Imato, *Angew. Chem. Int. Ed.* **2014**, *53*, 6993–6996.
[15] K. Chu, J. R. Adsetts, Z. Whitworth, S. Kumar, E. Zysman-Colman, Z. Ding, *Langmuir* **2023**, *39*, 2829–2837.
[16] P. Huang, B. Zhang, Q. Hu, B. Zhao, Y. Zhu, Y. Zhang, Y. Kong, Z. Zeng, Y. Bao, W. Wang, Y. Cheng, L. Niu, *ChemPhysChem* **2021**, *22*, 726–732.
[17] P. Huang, X. Zou, Z. Xu, Y. Lan, L. Chen, B. Zhang, L. Niu, *Molecules* **2022**, *27*, 7457.
[18] Y. Kong, Z. H. Zeng, P. Huang, Y. L. Luo, B. H. Zhang, L. J. Chen, Y. W. Zhang, D. X. Han, Y. X. Cheng, L. Niu, *Chin. J. Anal. Chem (Chinese: Fenxi Huaxue)* **2021**, *49*, 1015–1024.
[19] Z. Zeng, P. Huang, Y. Kong, L. Tong, B. Zhang, Y. Luo, L. Chen, Y. Zhang, D. Han, L. Niu, *Chem. Commun.* **2021**, *57*, 5262–5265.
[20] X. Wei, M.-J. Zhu, Z. Cheng, M. Lee, H. Yan, C. Lu, J.-J. Xu, *Angew. Chem. Int. Ed.* **2019**, *58*, 3162–3166.
[21] Y. Luo, B. Zhao, B. Zhang, Y. Lan, L. Chen, Y. Zhang, Y. Bao, L. Niu, *Analyst* **2022**, *147*, 2442–2451.
[22] C. Wang, J. Wu, H. Huang, Q. Xu, H. Ju, *Anal. Chem.* **2022**, *94*, 15695–15702.
[23] T. Hatakeyama, K. Shiren, K. Nakajima, S. Nomura, S. Nakatsuka, K. Kinoshita, J. Ni, Y. Ono, T. Ikuta, *Adv. Mater.* **2016**, *28*, 2777–2781.
[24] S. Madayanad Suresh, D. Hall, D. Beljonne, Y. Olivier, E. Zysman-Colman, *Adv. Funct. Mater.* **2020**, *30*, 1908677.
[25] a) D. Hall, S. M. Suresh, P. L. dos Santos, E. Duda, S. Bagnich, A. Pershin, P. Rajamalli, D. B. Cordes, A. M. Z. Slawin, D. Beljonne, A. Köhler, I. D. W. Samuel, Y. Olivier, E. Zysman-Colman, *Adv. Opt. Mater.* **2020**, *8*, 1901627;

b) L. Yang, L. Dong, D. Hall, M. Hesari, Y. Olivier, E. Zysman-Colman, Z. Ding, *SmartMat* **2023**, *4*, e1149.
[26] a) H. Zhou, Q. Ye, X. Wu, J. Song, C. M. Cho, Y. Zong, B. Z. Tang, T. S. A. Hor, E. K. L. Yeow, J. Xu, *J. Mater. Chem. C* **2015**, *3*, 11874–11880; b) M. Simard, D. Su, J. D. Wuest, *J. Am. Chem. Soc.* **1991**, *113*, 4696–4698.
[27] L. Yang, R. Zhang, B. Balónová, A. E. True, K. Chu, J. R. Adsetts, C. Zhang, X. Qin, E. Zysman-Colman, B. A. Blight, Z. Ding, *J. Electroanal. Chem.* **2022**, *920*, 116594.
[28] X. Liu, L. Li, L. Luo, X. Bi, H. Yan, X. Li, T. You, *J. Colloid Interface Sci.* **2021**, *586*, 103–109.
[29] N. Zhang, X.-T. Wang, Z. Xiong, L.-Y. Huang, Y. Jin, A.-J. Wang, P.-X. Yuan, Y.-B. He, J.-J. Feng, *Anal. Chem.* **2021**, *93*, 17110–17118.
[30] H. Hou, Y. Wang, Y. Wang, R. Luo, D. Zhu, J. Zhou, X. Wu, H. Ju, J. Lei, *J. Mater. Chem. C* **2022**, *10*, 14488–14495.
[31] L. S. Xie, G. Skorupskii, M. Dincă, *Chem. Rev.* **2020**, *120*, 8536–8580.
[32] a) Y. Hong, J. W. Y. Lam, B. Z. Tang, *Chem. Commun.* **2009**, 4332–4353; b) Y. Hong, J. W. Y. Lam, B. Z. Tang, *Chem. Soc. Rev.* **2011**, *40*, 5361–5388.
[33] X. Wei, M. J. Zhu, H. Yan, C. Lu, J. J. Xu, *Chem. Eur. J.* **2019**, *25*, 12671–12683.
[34] S. Carrara, A. Aliprandi, C. F. Hogan, L. De Cola, *J. Am. Chem. Soc.* **2017**, *139*, 14605–14610.
[35] L. Qian, B. Tong, J. Shen, J. Shi, J. Zhi, Y. Dong, F. Yang, Y. Dong, J. W. Y. Lam, Y. Liu, B. Z. Tang, *J. Phys. Chem. B* **2009**, *113*, 9098–9103.
[36] Y. Dong, J. W. Y. Lam, A. Qin, Z. Li, J. Sun, H. H. Y. Sung, I. D. Williams, B. Z. Tang, *Chem. Commun.* **2007**, 40–42.
[37] T.-B. Gao, J.-J. Zhang, R.-Q. Yan, D.-K. Cao, D. Jiang, D. Ye, *Inorg. Chem.* **2018**, *57*, 4310–4316.
[38] a) G. Jutz, P. van Rijn, B. Santos Miranda, A. Böker, *Chem. Rev.* **2015**, *115*, 1653–1701; b) L. Yang, D. Fan, Y. Zhang, C. Ding, D. Wu, Q. Wei, H. Ju, *Anal. Chem.* **2019**, *91*, 7145–7152.
[39] L. Yang, X. Sun, D. Wei, H. Ju, Y. Du, H. Ma, Q. Wei, *Anal. Chem.* **2021**, *93*, 1553–1560.
[40] Y. Gong, L. Zhao, Q. Peng, D. Fan, W. Z. Yuan, Y. Zhang, B. Z. Tang, *Chem. Sci.* **2015**, *6*, 4438–4444.
[41] B. Zhang, Y. Kong, H. Liu, B. Chen, B. Zhao, Y. Luo, L. Chen, Y. Zhang, D. Han, Z. Zhao, B. Z. Tang, L. Niu, *Chem. Sci.* **2021**, *12*, 13283–13291.
[42] J. M. Wong, R. Zhang, P. Xie, L. Yang, M. Zhang, R. Zhou, R. Wang, Y. Shen, B. Yang, H.-B. Wang, Z. Ding, *Angew. Chem. Int. Ed.* **2020**, *59*, 17461–17466.
[43] M. Hesari, Z. Ding, *Nat. Protoc.* **2021**, *16*, 2109–2130.
[44] T. Han, Y. Cao, J. Wang, J. Jiao, Y. Song, L. Wang, C. Ma, H. Y. Chen, J. J. Zhu, *Adv. Funct. Mater.* **2023**, *33*, 2212394.

Manuscript received: May 12, 2023
Accepted manuscript online: June 21, 2023
Version of record online: ■■, ■■

REVIEW

This review summarizes recent advances towards enhanced electrochemiluminescence (ECL) using novel design strategies such as thermally activated delayed fluorescence (TADF) luminophores (both donor-acceptor and multiresonance), hydrogen-bonding complexes, and aggregation- and crystallization-induced emission strategies. In many scenarios, the ECL enhancement is shown to be significant, thus suggesting future applications for thin film optoelectronics and sensing. These new avenues of intelligent ECL luminophore designs are expected to be of great importance for ECL-related research.

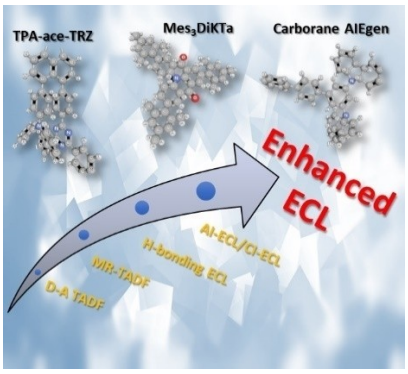

K. Chu, Prof. Dr. Z. Ding, Prof. Dr. E. Zysman-Colman**